

---

# Heterogeneous Federated Learning

---

Fuxun Yu<sup>1</sup>, Weishan Zhang<sup>1</sup>, Zhuwei Qin<sup>1</sup>, Zirui Xu<sup>1</sup>  
Di Wang<sup>2</sup>, Chenchen Liu<sup>3</sup>, Zhi Tian<sup>1</sup>, Xiang Chen<sup>1</sup>

<sup>1</sup>George Mason University, <sup>2</sup>Microsoft

<sup>3</sup>University of Maryland, Baltimore County

{fyu2, wzhang23, zqin, zxu21, ztian1, xchen26}@gmu.edu  
wangdi@microsoft.com, ccliu@umbc.edu

## Abstract

Federated learning learns from scattered data by fusing collaborative models from local nodes. However, due to chaotic information distribution, the model fusion may suffer from structural misalignment with regard to unmatched parameters. In this work, we propose a novel federated learning framework to resolve this issue by establishing a firm structure-information alignment across collaborative models. Specifically, we design a feature-oriented regulation method ( $\Psi$ -Net) to ensure explicit feature information allocation in different neural network structures. Applying this regulating method to collaborative models, matchable structures with similar feature information can be initialized at the very early training stage. During the federated learning process under either IID or non-IID scenarios, dedicated collaboration schemes further guarantee ordered information distribution with definite structure matching, so as the comprehensive model alignment. Eventually, this framework effectively enhances the federated learning applicability to extensive heterogeneous settings, while providing excellent convergence speed, accuracy, and computation/communication efficiency.

## 1 Introduction

Federated Learning (FL) has drawn great attention with outstanding collaborative training performance and data privacy supportability [6]. It is commonly achieved by fusing collaborative nodes' homogeneous neural networks through Federated Averaging (FedAvg), which generates a global model by averaging local parameters with the same coordinates [6, 13]. However, FedAvg suffers from non-negligible accuracy drop due to inevitable heterogeneity: highly Non-IID data across nodes may cause huge divergence within the parameters to be averaged and thus significantly skewed results [18, 4].

Recent works further elaborate on such heterogeneity from a structural alignment perspective [7, 2, 12]. Although local neural network models have the homogeneous architecture, the parameters with the same model coordinates might learn different features at different levels, resulting in chaotic parameter distribution across collaborative nodes. Therefore, the conventional coordinates-based averaging scheme might fuse unmatched parameters and continuously hurt the global convergence [13, 15].

Several Federated Learning optimization works have been proposed to leverage this structural alignment property (*i.e.*, "permutation invariance" [13]), such as Representation Matching [7], Bayesian Matching [16], FedMA [13], *etc.* They conform to a common methodology: after a certain amount of local training, they evaluate parameter similarity across local models and reorganize the permutation, so that approximate parameters could be averaged together. Although outperformed conventional schemes like FedAvg, these methods still have certain limitations, such as inaccurate parameter matching, extra computation/communication overhead, limited heterogeneous applicability, and compromised data privacy.

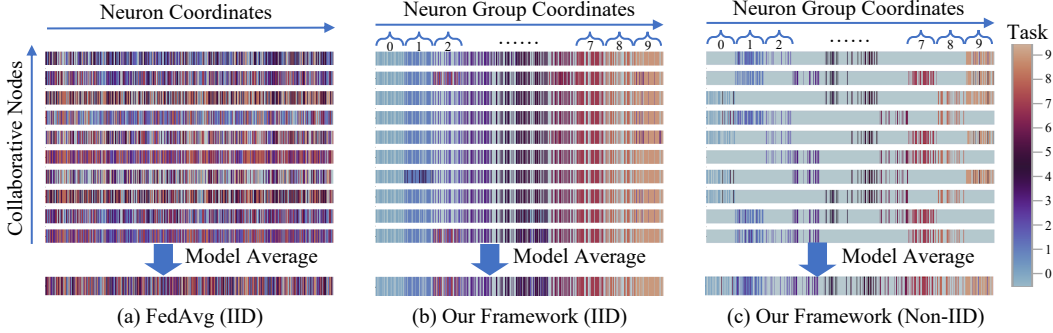


**Figure 1:** The feature encoding comparison between FedAvg and our proposed framework. The color of each neuron is determined by its top response class to indicate its learned feature, as defined in Eq. 2. **(a)** The original FedAvg with chaotic feature encoding can suffer from feature averaging conflicts among different nodes. **(b) & (c)** In contrast, our framework enforces structurally-aligned feature encoding and alleviates such averaging conflicts in both IID and non-IID cases. Experiments are conducted with 10 collaborative nodes (VGG9 on CIFAR10). IID: Each node has data of 10 classes. Non-IID: Each node has data of 5 varied classes.

To tackle these limitations, we propose a novel FL framework to resolve this issue by establishing not only structure but also information alignment across collaborative models. Specifically, we design a feature-oriented regulation method ( $\Psi$ -Net), which can effectively identify local models’ structural hierarchies and grouped components that are associated with particular classes and corresponding features. Based on such explicit feature information allocation, matchable structures with similar feature information can be initialized at the very early training stage, and further guarantees ordered information distribution with definite structure matching along the whole training process. Fig. 1 provides a set of intuitive comparisons for parameter matching across collaborative models. With the proposed feature allocated regulation, our model’s encoded feature distribution conform to structural alignments with corresponding classes, while regular FedAvg’s model fusion suffers from significant parameter mismatching and therefore expected performance degradation.

We conduct extensive experiments on general datasets (CIFAR10, 100) with two model architectures to regulate (VGG16 and MobileNet). Our work demonstrates significant improvement in both convergence speed and accuracy, outperforming previous state-of-the-art works by large margins (+2.5%~4.6%) with significantly less computation and communication cost. Especially under highly-skewed non-IID scenarios, our work still performs effective and robust model alignment to facilitate the convergence while most previous methods cannot. To our best knowledge, this is the very first work that solves the FL alignment problem directly from a model regulation perspective, which significantly improves the FL applicability in various heterogeneous settings.

## 2 Background and Motivation

**Neural Network Permutation Invariance.** From a permutation perspective, the model parameters (*e.g.*, neuron weight matrix  $\Omega_i$  in the *i*th node’s model) can be decoupled as  $\omega_i \Pi_i$ , where  $\omega_i$  defines parameter values and  $\Pi_i$  defines the alignment sequence. For  $N$  collaborative training nodes with the homogeneous neural network architecture, the model permutation invariance can be formulated as:

$$F(X) = (\omega_0 \Pi_0) \Pi_0^T X = \dots = (\omega_i \Pi_i) \Pi_i^T X = \dots = (\omega_N \Pi_N) \Pi_N^T X. \quad (1)$$

Although the local models across collaborative nodes can achieve the same global function  $F$  on the input set  $X$ , the local models’  $\omega$  and  $\Pi$  can vary from model to model [13, 15]. In such circumstances, their encoded feature distribution can vary due to the permutation matrix  $\Pi$ , causing considerable parameter mismatching ( $\omega_i \Pi_i \neq \omega_j \Pi_j$ ) and thus collaborative training performance degradation.

**Matched Averaging with Permutation Adjustment.** To achieve FL model alignment, previous methods mainly improve FedAvg by iteratively matching approximate parameters with permutation adjustment before each global averaging cycle. Their common approach is to first identify approximate parameters by evaluating certain parameter characteristics (*e.g.*, weight value or activation degree) across collaborative nodes based on a similarity metric (mostly *MSE* loss). Then, they will search an adjustment matrix  $\Pi_i^{trans}$  for reordering to achieve the minimum divergence with the averaging target:  $\omega_i \Pi_i \Pi_i^{trans} \approx \omega_j \Pi_j$ . Specifically, such a problem can be resolved by optimization algorithms similar to solving the Wasserstein Barycenter problem [11].

**Limitations of the State of the Art.** Although the current parameter matching works alleviated the FL model alignment issue, they still suffer from certain limitations:

- (1) *Inaccurate Parameter Matching*: The state of the art’s (SOTA) structural alignment accurateness is limited by the quantitative parameter similarity evaluation. The parameters with the least *MSE* difference in weight/activation may carry distinct feature information, and therefore the forced matching without qualitative verification can cause catastrophic information loss [5, 9];
- (2) *Heterogeneous Applicability*: SOTA assumes different local models have mostly matchable parameters ( $\omega_i \approx \omega_j$ ). While the practical FL heterogeneity may involve highly Non-IID local data and even asymmetric learning tasks, leading huge model alignment complexity [7, 4];
- (3) *Performance Overhead*: The post-training parameter matching incurs extra computation load for parameter similarity evaluation and permutation adjustment optimization. Meanwhile, parameter similarity evaluation across nodes also introduces considerable communication overhead;
- (4) *Data Privacy*: Moreover, the activation-based similarity evaluation requires data sharing between different nodes, thus the data privacy can be compromised [11].

**Design Motivation: Feature-Level Alignment.** We expect to relieve the above problems from two aspects: On one hand, beyond feature-agnostic parameter similarity evaluation, we would further interpret the encoded feature information in neural network components and promote the parameter similarity assessment to the feature level. On the other hand, we would design a feature-oriented model regulation method to ensure explicit feature allocation in specific model structures. Rather than post-training alignment, such a regulation method adjusts local model architecture according to their data and task distribution at the very early training stage, and continuously maintain not only structure but also information alignment for better FL performance.

Motivated by these two aspects, our work begins with the interpretation of encoded feature information in neural networks. Specifically, we adopt a neuron’s class response preference to indicate its learned feature [9, 8, 10, 19]: Starting with single fully-connected layer for classification tasks, such a preference can be measured by observing the neuron’s activation response  $A(x_c)$  on inputs  $x$  from  $C$  classes, as well as its gradients  $\partial Z_c / \partial A(x_c)$  (or weights  $w_c$  equally) towards a class  $c$ ’s prediction confidence  $Z_c$ . Combining these two factors and further generalizing to a multi-layer convolutional neural network, a neuron’s learned feature can be indicated by its class preference vector:

$$P = [p_1, \dots, p_c, \dots, p_C], \quad \text{where } p_c = \sum_b^B A(x_{c,b}) * \frac{\partial Z_c}{\partial A(x_{c,b})}, \quad (2)$$

where  $A(x_{c,b})$  denotes activations and  $\partial Z_c / \partial A(x_{c,b})$  denotes gradients from class  $c$ ’s confidence, both of which are averaged on  $B$  batch trials. The effectiveness of such an interpretation approach is illustrated in Fig. 1, which demonstrates the parameter/feature divergence from a functionality perspective and highlights the advantages of our feature-level structural information alignment.

**Our Work: Feature-Allocated Model Regulation and Collaboration.** Based on the feature interpretation, our major work focuses on the second motivation aspect. Specifically, we propose a novel federated learning framework including feature-regulated model design and a set of robust collaboration policies under various heterogeneous settings. Fig. 2 presents the framework overview. Leveraging feature distribution exploration with Eq. 3, we designed a  $\Psi$ -Net model structure that consists of shared layers and grouped layers, which are expected to share fundamental features with all learning classes and isolate class-specific features within exclusive structures, respectively. By regulating existing model architectures into such a  $\Psi$ -Net structure, we can maintain features’ consistent structural allocation in different training stages, and thereby establishing the basis for the feature level model alignment. The collaboration policies can further specify the optimal  $\Psi$ -Net configuration and particular model fusion schemes for various FL scenarios. Not only capable for regular IID and non-IID data distribution, our framework can even support extreme heterogeneous cases, where certain classes might be unlearnable on particular collaborative nodes. Eventually, this framework is expected to effectively enhance the FL applicability to extensive heterogeneous settings, while providing excellent convergence speed, accuracy, and computation/communication efficiency.

### 3 $\Psi$ -Net Structure for Feature Allocation

#### 3.1 Feature Allocation Definition

For a given neural network, the goal of feature allocation can be defined by a structure-feature mapping relationship ( $M$ ) between the model meta-structure sets ( $S$ ) and task sets ( $T$ ):

$$M = \{s_i^t : t \text{ or } \langle t_0, \dots, t_n \rangle\}, \quad \text{s.t. } \forall i \neq j, M(s_i) \cap M(s_j) = \emptyset, \quad (3)$$

where  $s_i^t$  indicates one meta-structure (e.g., one set of neurons in the neural network) mapped to one (or one set of) task feature  $t$ , and  $M(s^{t1}) \cap M(s^{t2}) = \emptyset$  enforces that any individual task feature can be assigned to only one meta-architecture.

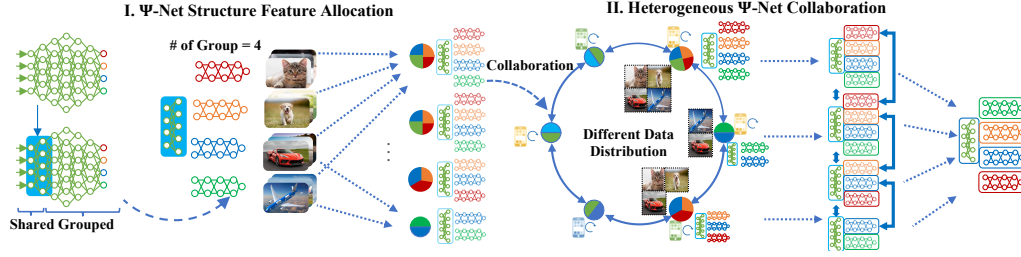


**Figure 2:** Our proposed heterogeneous learning framework includes two major steps: **(I)** We utilize group-convolution based  $\Psi$ -net structure as a regulation for feature allocation. **(II)** Then we propose the heterogeneous  $\Psi$ -net FL policy by grouped-shared parameter averaging to handle both IID and non-IID data distributions.

In general, due to the insufficient interpretability, it’s hard to either find the meta-structure  $s_i$  or interpret the feature  $t$  in a convolutional neural network, not to mention manipulating its feature encoding mapping. But interestingly, the AlexNet authors found that AlexNet learns distinct shape-oriented and color-oriented features in its two separated convolution groups [1], so did ShuffleNet [17] with their findings that features become biased among different convolutional groups. The two networks both utilize the group convolution structure. Although for different purposes, they demonstrate the similar feature regulation effects. Following such observation, our hypothesis is in the densely-connected convolutional structures, the training gradients carrying task features can usually backpropagate through the entire network, leading to random feature encoding orders. In contrast, the group convolution separates different groups and build implicit boundaries between them, thus preventing gradients flowing interleaved and achieving certain feature regulation effects.

From this perspective, we propose our  $\Psi$ -net regulation utilizing grouped convolutional and linear layers to build a meta-structure sets  $S$ . Meanwhile, by allocating the class logit  $t$  to the structure group  $s_i$ , we assume that the feature of task  $t$  is also allocated to the structure,  $s_i \rightarrow s_i^t$ . In this way, the meta-structure  $s_i^t$  always acts as the feature anchor for task feature  $t$  regardless of on which nodes  $i$ , thus ensuring the feature alignment within structure  $s^t$  among all nodes:

$$\Omega_t \leftarrow s_i^t \approx \dots s_j^t \approx \dots s_N^t, \quad \forall i, j \in N. \quad (4)$$

Meanwhile, even though different nodes can have varied structure orders, their local structure  $s_i^t$  can still be explicitly mapped with the  $\Omega_t$ , which is the  $t$ -th meta-structure in the global model structure  $\Omega$ . With such a feature alignment property, we are then able to enforce the structural feature alignment and achieve even heterogeneous model collaboration, as we will show later.

### 3.2 $\Psi$ -Net Structure Implementation

As shown in Fig. 2 (a),  $\Psi$ -Net structure regulation is composed of two major parts to achieve grouped-based feature allocation: Non-grouped shared layers (lower convolutional layers) and grouped layers (higher convolutional and fully-connected layers).

**Shared Layers.** The design of shared layers is due to the shallow layers learn mostly basic features that are useful for most tasks and show less feature divergence. In such cases, grouping these layers can prevent neurons in one group from receiving gradients from other groups, leading to sub-optimal learning performance. Therefore, the shallow layers are reserved shared without grouping.

To determine an appropriate number of shared layers to reserve, we evaluate the feature divergence of layer  $l$  based on the total variance ( $TV$ ) of neurons’ feature encoding:

$$TV_l = \sum_i^L \frac{1}{L} \|P_{l,i} - E(P_{l,i})\|_2, \quad \text{where } P_{l,i} = [p_{l,1}, \dots, p_{l,c}, \dots, p_{l,N}] / \sum_j^N p_{l,j}, \quad (5)$$

where we use the neuron’s class preference vector  $P_{l,i}$  in Eq. 2 as an indication of its learned feature.

From shallow to deep layers, the layer-wise feature divergence can surge to high points in some medium levels. We thus evaluate the feature divergence and empirically determine a sharing depth to start the grouped layer construction. In later experiments, we will evaluate our depth selection and show that our  $\Psi$ -net structure is fairly robust to the depth hyper-parameter selection.

**Group Convolutional Layers.** For the deeper convolutional layers, the encoded class feature are more diverged and thus easier to conflict with each other during weight averaging. Therefore, we utilize group convolution and construct separable group convolutions. In each group, the convolutional neuron can only receive/output the feature channels within the current group. Thus, the backpropagated gradients carrying feature information can only flow through the individual group, avoiding the feature interleaving between different groups.

Considering the practical training dataset complexity, the number of groups cannot be always “one-to-one” matched to the training tasks. Therefore, on big datasets (*e.g.*, CIFAR100 with 100 classes), we also supports “one-to-many” mapping, *i.e.*, multiple class logits mapped to one convolutional group, so as to achieve high scalability but without sacrificing the feature regulation performance too much. As we will show later, both one-to-one mapping on small datasets (CIFAR10) and one-to-many mapping on mediate datasets (CIFAR100) can achieve as good structural feature regulation benefits.

**Grouped Fully-Connected Layers.** For the fully-connected (FC) layers, the previous FC layers often connect all input convolutional neurons to the class logits, and thus cannot regulating which convolutional group learns the corresponding task features. In  $\Psi$ -net, we also decouple the original FC layer into groups, *i.e.*, multiple linear layers with same number as the convolutional groups. One linear layer connects the class logit(s) with the mapped convolutional groups only, thus enforcing the gradients flowing backwards to the mapped group without any leakage. Multi-layer FC layers can be decoupled similarly across layers, which we omit for simplicity.

**Group Normalization Layers.** Previous works have shown that batch normalization layers can influence the FL performance as different local models tend to collect non-consistent batch mean and variance statistics (especially in non-IID cases), thus degrading the performance [4]. Our  $\Psi$ -net structure design, by enforcing the similar feature encoding, alleviates the batch statistics divergence within each group. Therefore, we propose to incorporate the Group Normalization (GN) layer [14] into our  $\Psi$ -net structure to improve the model convergence performance. Specifically, we add the GN layer after each grouped convolutional layer, both with the same number of groups to ensure the batch statistic normalization is conducted within each group. For the shared layers, we can regard it as a layer with group number equal to 1, which deduces to the normal batch normalization. In the later evaluation, we will demonstrate the effectiveness of GN in our  $\Psi$ -net structure.

Overall, by our  $\Psi$ -net structure, we can isolate different convolutional groups, so as the task features between them. Each conv/fc group only learns the specified task features from the assigned class logits by gradient back-propagation, enabling a pre-aligned feature allocation during local training. Also,  $\Psi$ -net regulation is highly configurable and supports dynamic structure-feature mapping, which provides high flexibility in handling training datasets with different complexity.

#### 4 $\Psi$ -Net Collaboration for Heterogeneous Federated Learning

In this section, we present the particular FL collaboration framework based on the  $\Psi$ -Net structure regulation through different training stages. To demonstrate the framework’s applicability for various heterogeneous settings, we target both IID and non-IID data distribution scenarios. Especially, we also take an extreme non-IID case into consideration: certain classes’ data volume might be too small or missing on particular nodes, resulting in asymmetric learning tasks across local models.

**Global & Local Model Initialization.** Regarding the heterogeneity across collaborative nodes, the  $\Psi$ -Net based global and local models might be initialized differently for training scenario adaptation.

*Global Model:* Given a global task with multiple learning classes and a target neural network architecture to transform (*e.g.*, VGG16), the proposed regulation method will first identify the depth boundary between shared and grouped layers based on Eq. 5. Regardless of IID or non-IID scenarios, the number of separated layer groups will be determined with the mapping schemes described in Sec. 3 to guarantee the expected granularity and scalability with different learning class volumes.

*Local Model:* In IID and general non-IID data distribution cases, local models share the homogeneous structure with the global model. While in the extreme non-IID cases, where particular nodes are unable to learn certain classes, heterogeneous models will be initialized for the asymmetric learning tasks. From the structure-information alignment perspective, the structure groups corresponding to unlearnable classes will be trimmed, as they cannot learn useful information to contribute.

Such a trimming process is implemented differently following the mapping scheme adopted by the global model: With the “one-to-one” mapping scheme, any structure group without local task data being present would be trimmed. While with “one-to-many”, the trimming of one structure group is conducted only if all the mapped tasks  $M(s_c)$  are not present in node  $i$ ’s local data  $LD(i)$ :

$$s_c = \mathbf{1}, \text{ iff } M(s_c) \cap LD(i) = \emptyset, \text{ otherwise } \mathbf{0}, \quad (6)$$

where  $M(s_c)$  is the task set mapped to the current conv/fc group. Better rules may be determined considering the amount of data or abandoning isolated classes, which we leave as future work.

**Local Model Training.** Local training is conducted epoch-wise as regular FL schemes. However, different from SOTA, the structure-information alignment is continuously guaranteed without consid-

erable overheads, such as parameter sharing, evaluation, and post-training alignment. Moreover, the nodes with asymmetric tasks further trim local models, leading to less computation cost.

**Aligned Model Averaging.** The averaging will be conducted periodically every  $e$  epochs.

*Shared layers* will be synchronized by local models from all  $N$  collaborative nodes. As they extract fundamental features with less class-specific divergence, an global averaging can be directly applied:

$$\Omega_{shared} = Avg(\omega_{shared}^i), \quad i \in \{1, \dots, N\}, \quad (7)$$

where  $\omega_{shared}^i$  denotes the weights of the shared layers from the  $i$ th node’s local model. Moreover, such uniformed shared layers also benefit for global consensus under heterogeneous scenarios.

*Grouped layers* conduct model averaging only within matched groups, which are supposed to have the same primary learning class to alleviate potential feature conflicts:

$$\Omega_c = Avg(\omega_c^{\mathbf{I}_c}), \quad \text{where } \mathbf{I}_c = \{i, \text{ s.t. } c \in M(i)\}, \quad (8)$$

where  $\Omega_c$  denotes the averaged weights of the grouped layer structures for the  $c$ th learning class,  $\mathbf{I}_c$  indicates the indices of collaborative nodes where class  $c$  presents in their local data sets. Ideally, all collaborative nodes should be included in  $\mathbf{I}_c$ . However, when asymmetric learning tasks occur,  $\mathbf{I}_c$  will exclude certain unsupportive local models for class  $c$ .

*Normalization layers*, including batch and group normalization layer, are averaged in a similar way: For batch normalization in shared layers, we average the “*shift*” and “*scale*” parameters, as well as the the “*running\_mean*” and “*running\_variance*” statistics for each layer. For group normalization in the grouped layers, only the “*shift*” and “*scale*” parameters are averaged within matched groups, as the other two are subject to the batch change.

**Heterogeneous Model Collection.** Taking the aforementioned extreme non-IID cases into consideration, the final global model can be considered as a collection of heterogeneous local structures:

$$\Omega^{Global} = \{\Omega_{shared}, \Omega_1, \dots, \Omega_C\}. \quad (9)$$

Overall, along with the feature allocated structure regulation, our framework can avoid the collaborative conflicts and achieve continuously feature alignment regulation during different FL stages. In next section, we conduct systematical evaluation of our framework.

## 5 Experiment

**Experiment Setup.** We evaluate our proposed framework with image classification tasks on CIFAR10 and CIFAR100. Three neural network architecture, namely VGG9, VGG16, and MobileNetV1, are adopted to demonstrate the generality of our structure regulation method. For local data distributions, we consider both IID and non-IID scenarios, where the non-IID can have only partial classes of the dataset. State-of-the-art works including FedMA [13] and FedProx [3] are compared to demonstrate the efficiency and effectiveness of our proposed framework. Code will be released.

### 5.1 Convergence Performance Improvement Evaluation

In this section, we first demonstrate our framework’s advanced performance in terms of convergence accuracy and speed. As aforementioned, we adopt the “one-to-one” mapping scheme to generate 10 structure groups with  $\Phi$ -Net on CIFAR10 for fine-grained feature allocation. On CIFAR100, we also utilize the 10-group structure with the “one-to-many” mapping in order to achieve the required scalability with increased dataset complexity.

**Accuracy Improvement (Non-IID to IID).** We demonstrate our framework’s full-spectrum accuracy improvement in Table. 1. The experimental setting  $N * C$  indicates there are  $N$  collaborative nodes, and each node has  $C$  classes present in the local data distribution. The global dataset is split randomly and equally onto different nodes without any duplication. The results reveal that our framework consistently outperforms the baseline – FedAvg by **+1%~4%** accuracy on VGG9. FedAvg on MobileNetV1 seems to suffer more from the highly-skewed non-IID data distribution. As a result, our framework could achieve **+6%~19%** accuracy on MobileNetV1.

**Accuracy Improvement (Node Scalability).** Similar experiments are conducted to evaluate our framework’s generality with node scaling. Specifically, we scale the number of collaborative nodes from 10 to 100 with the non-IID data distribution (each node only have 5 classes present in the local data distribution). Without loss of generality, our framework provides consistently better performance ranging from **+2%~4%** on VGG9 and **+5%~11%** on MobileNetV1.

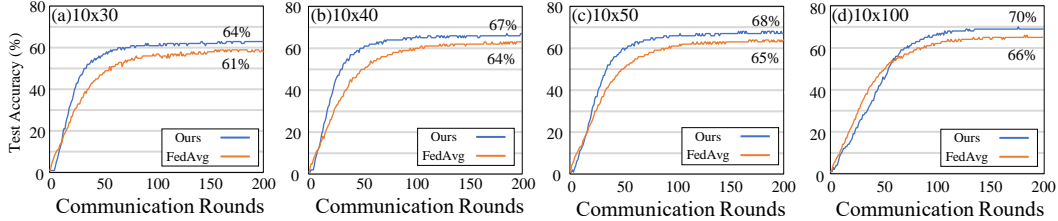
The underlying reasons of our accuracy improvement is due to the structurally aligned feature distribution across local models, as demonstrated in Fig. 1. Such feature alignment alleviates the

**Table 1: Non-IID Spectrum (CIFAR10).**

N * C		10x3	10x4	10x5	10x10
VGG9	FedAvg	82%	84%	85%	88%
	Ours	83%	88%	88%	90%
MbNet	FedAvg	67%	71%	79%	85%
	Ours	86%	88%	90%	91%

**Table 2: Node Scalability (CIFAR10).**

N * C		10x5	20x5	50x5	100x5
VGG9	FedAvg	85%	86%	83%	83%
	Ours	88%	88%	86%	87%
MbNet	FedAvg	79%	85%	81%	78%
	Ours	90%	90%	89%	88%

**Figure 3: Convergence Speed Comparison between FedAvg and Proposed Method (VGG16 on CIFAR10).**

parameter averaging conflicts and providing higher convergence accuracy. This also benefits the convergence speed as discussed in the next section.

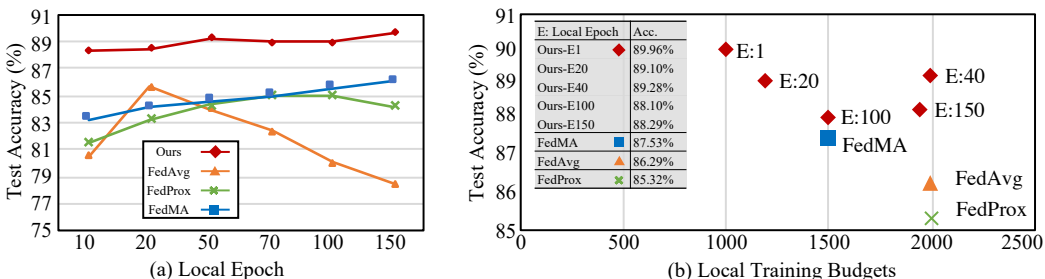
**Convergence Speed Improvement.** Four settings are selected similar with CIFAR10 non-IID spectrum settings, *e.g.*, 10 nodes with each node having partial classes presented. Fig. 3 shows the test accuracy curves of FedAvg and ours through the entire training process. In all the non-IID cases, our method consistently shows higher convergence speed with only 50-80 rounds for the optimal performance, while FedAvg usually needs at least 100 rounds. One exception is the 10x100 IID setting, the initial convergence of FedAvg seems to be faster, but our method soon exceeds it after 50 epochs and finally achieves +4% accuracy than FedAvg.

## 5.2 Performance Comparison with SOTA (FedProx & FedMA)

In this part, we conduct performance comparison between our work with SOTA methods including FedProx and FedMA. We compare our performance in two aspects: (1) convergence accuracy under different local training epoch numbers  $e$ ; (2) the optimal performance under given local training budgets. The overall results are shown in Fig. 4, where the SOTA results are referred from [13]. All experiments use the same setting (VGG9, 16 nodes) with the dirichlet data distribution of CIFAR10.

**Communication Efficiency with Different Local Epochs.** As previous work studied, with higher local training epochs, the frequency of the communication in FL could be effectively reduced. However, longer local training epochs can also lead to sub-optimal performance, since the model collaboration are less frequent with potential model divergence. Therefore, we aim to achieve high convergence accuracy with as longer local epochs as possible. Fig. 4 (a) shows the convergence accuracy performance comparison under local epoch settings  $\{10, 20, 50, 70, 100, 150\}$ . All models are trained with 54 averaging rounds as per settings in [13] for fair comparison. Clearly, our framework shows the best performance under all settings, improving FedMA by +3%~5% accuracy.

**Computational Efficiency with Local Training Budgets.** Specifically, the results of baseline FedAvg and SOTA works are their corresponding optimal performance reported in [13]. As we can see that, our method could achieve +0.6%~2.4% accuracy than FedMA with similar or less local training budgets. For FedAvg and FedProx, our method could achieve +3.0% and +4.0% accuracy improvement with the same training budget, respectively.

**Figure 4: Local Epoch Influence and Local Training Budgets Comparison with SOTA.**

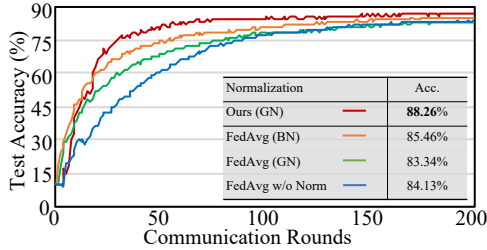


Figure 5: Normalization Strategy Analysis.

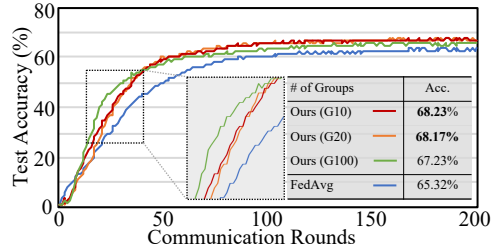


Figure 6: Number of Groups Analysis.

### 5.3 Ablation Study of Design Components

We study the performance influence of three design strategies in our framework, including the normalization layer influence, grouping number selection, as well as the sharing layer depth selection.

**Normalization Strategy Analysis.** For normalization strategy analysis, we compare our work and FedAvg under the data distribution of (VGG9, CIFAR10, 10x4 non-IID). The results are shown in Fig. 5. The baseline FedAvg without normalization achieves 84.13% accuracy. FedAvg+BN helps improve the accuracy to 85.46%, while FedAvg+GN hurts the model performance, degrading the accuracy to 83.34%. Utilizing the same GN settings, our work instead achieves the best accuracy 88.26%. This further demonstrates that our grouped structure helps alleviate the statistics divergence within groups, thus the group normalization could benefit the model performance.

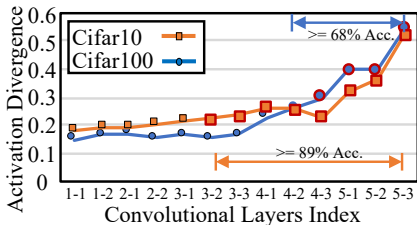
**Grouping Number Analysis.** In this part, the performance robustness of our model is demonstrated with complementary benefits under different group number selection. The overall results are shown in Fig. 6 (VGG16, CIFAR100, 10x50 non-IID). Our 10-group and 20-group structures both achieve the optimal performance around  $\sim 68\%$ , providing +2.7% accuracy improvement than FedAvg – 65.3% with the original structure. The 100-group structure, though achieving sub-optimal accuracy improvement (+1.9% than FedAvg), shows the highest convergence speed (the green curve). We hypothesize the convergence speedup is brought by its most fine-grained feature alignment benefits (1 class mapped to 1 group). But oppositely, with 100 groups, the per-path capacity can be limited. Though sub-optimal accuracy, it verifies the group size trade-off as discussed in Sec. 3.

**Grouping Depth Analysis.** We also demonstrate that our framework’s performance is robust to the grouping depth hyper-parameter selection in Figure 7. Specifically, our model shows nearly optimal performance 89%~90% in large ranges of depth selection, *e.g.*, from C3-2 to C5-2 on CIFAR10. Also, the total variance of the model (a pre-trained model with minimum 50 epoch pre-training) offers good indication of the layer-wise feature divergence.

## 6 Conclusion

In this paper, we proposed a novel federated learning framework to resolve FL models’ chaotic fusion problem by establishing a firm structure-information alignment. In the process of proposing this method, we adopted feature-oriented parameter interpretation and proposed a novel feature-oriented regulation method ( $\Psi$ -Net) to ensure explicit feature information allocation in different neural network structures. Such a regulation method adjusts the local model architecture according to their data and task distribution at the very early training stage, and continuously maintain not only structure but also information alignment for better FL performance. To our best knowledge, this is the very first work that solves the FL alignment problem directly from a model regulation perspective, which significantly improves the FL performance and applicability in various heterogeneous settings.

Figure 7 & Table 3: Grouping Depth Sensitivity. **Left:** Total Variance of each layer. **Right:** Performance under different grouping depth, showing our models’ performance is robust to depth selection (10x5, 10x50 non-IID).



VGG16	C1-2	C2-2	C3-2	C4-2	C5-2	FC	None
CIFAR10	82%	87%	89%	90%	89%	87%	86%
CIFAR100	53%	62%	67%	68%	69%	68%	65%



## References

- [1] Alex Krizhevsky, Ilya Sutskever, and Geoffrey E Hinton. Imagenet classification with deep convolutional neural networks. In *Advances in neural information processing systems*, pages 1097–1105, 2012.
- [2] M. I. Leontev, V. Islenteva, and S. V. Sukhov. Non-iterative knowledge fusion in deep convolutional neural networks. *Neural Processing Letters*, 51(1):1–22, 2020.
- [3] T. Li, A. K. Sahu, M. Zaheer, M. Sanjabi, A. Talwalkar, and V. Smith. Federated optimization in heterogeneous networks. In *Proceedings of the 3rd MLSys Conference*, 2018.
- [4] X. Li, K. Huang, W. Yang, S. Wang, and Z. Zhang. On the convergence of fedavg on non-iid data. In *Proceedings of the 8th International Conference on Learning Representations (ICLR)*, 2019.
- [5] Z. Liu, M. Sun, T. Zhou, G. Huang, and T. Darrell. Rethinking the value of network pruning. In *Proceedings of the 7th International Conference on Learning Representations (ICLR)*, 2019.
- [6] H Brendan McMahan, Eider Moore, Daniel Ramage, Seth Hampson, et al. Communication-efficient learning of deep networks from decentralized data. *arXiv preprint arXiv:1602.05629*, 2016.
- [7] H. Mostafa. Robust federated learning through representation matching and adaptive hyper-parameters. *arXiv preprint:1912.13075*, 2019.
- [8] Z. Qin, F. Yu, C. Liu, and X. Chen. How convolutional neural network see the world—a survey of convolutional neural network visualization methods. *arXiv preprint:1804.11191*, 2018.
- [9] Z. Qin, F. Yu, C. Liu, and X. Chen. Functionality-oriented convolutional filter pruning. In *Proceedings of 30th British Machine Vision Conference (BMVC)*, 2019.
- [10] W. Samek, A. Binder, G. Montavon, S. Lapuschkin, and K. Müller. Evaluating the visualization of what a deep neural network has learned. *IEEE transactions on neural networks and learning systems*, 28(11):2660–2673, 2016.
- [11] S. P. Singh and M. Jaggi. Model fusion via optimal transport. *arXiv preprint:1910.05653*, 2019.
- [12] J. Smith and M. Gashler. An investigation of how neural networks learn from the experiences of peers through periodic weight averaging. In *Proceedings of the 16th IEEE International Conference on Machine Learning and Applications (ICMLA)*, pages 731–736. IEEE, 2017.
- [13] H. Wang, M. Yurochkin, Y. Sun, D. Papailiopoulos, and Y. Khazaeni. Federated learning with matched averaging. In *Proceedings of the 8th International Conference on Learning Representations (ICLR)*, 2020.
- [14] Yuxin Wu and Kaiming He. Group normalization. In *Proceedings of the European Conference on Computer Vision (ECCV)*, pages 3–19, 2018.
- [15] M. Yurochkin, M. Agarwal, S. Ghosh, K. Greenewald, N. Hoang, and Y. Khazaeni. Probabilistic federated neural matching. 2018.
- [16] M. Yurochkin, M. Agarwal, S. Ghosh, K. Greenewald, T. N. Hoang, and Y. Khazaeni. Bayesian nonparametric federated learning of neural networks. In *Proceedings of the 36th International Conference on Machine Learning (ICML)*, pages 7252–7261, 2019.
- [17] Xiangyu Zhang, Xinyu Zhou, Mengxiao Lin, and Jian Sun. Shufflenet: An extremely efficient convolutional neural network for mobile devices. In *Proceedings of the IEEE conference on computer vision and pattern recognition*, pages 6848–6856, 2018.
- [18] Yue Zhao, Meng Li, Liangzhen Lai, Naveen Suda, Damon Civin, and Vikas Chandra. Federated learning with non-iid data. *arXiv preprint arXiv:1806.00582*, 2018.
- [19] B. Zhou, A. Khosla, A. Lapedriza, A. Oliva, and A. Torralba. Learning deep features for discriminative localization. In *Proceedings of Computer Vision and Pattern Recognition (CVPR)*, pages 2921–2929, 2016.